TE- and TM-polarized roughness-assisted free-carrier absorption in quantum wells at midinfrared and terahertz wavelengths

I. Vurgaftman and J. R. Meyer
Code 5613, Naval Research Laboratory, Washington, D.C. 20375
(Received 17 May 1999)

A free-carrier absorption mechanism, in which a photon transition is accompanied by an elastic interface-roughness scattering event, is considered for a few representative quantum well structures. Interface-roughness scattering determines the low-temperature mobility in undoped narrow quantum wells such as those used in infrared lasers. It is found that in spite of the contribution due to scattering to higher subbands, the absorption coefficient for TE-polarized light remains appreciably less than the semiclassical value at shorter wavelengths. The implications of these results for the recently proposed interband far-infrared and terahertz lasers based on ''*W*'' antimonide structures are discussed. In the case of roughness-assisted absorption of TM-polarized light, transitions forbidden by symmetry and exclusion arguments become allowed. However, the largest second-order contribution relative to first-order intersubband absorption tends to occur at wavelengths where the total absorption coefficient is rather small. [S0163-1829(99)10143-7]

I. INTRODUCTION

Quantum wells currently form an integral part of many optoelectronic devices, e.g., serving as active regions in semiconductor lasers. Near-infrared laser diodes are well established and have demonstrated high-power cw operation at room temperature and differential quantum efficiencies close to unity. On the other hand, the development of midinfrared (mid-IR) semiconductor lasers remains ongoing,[1,2] and the feasibility of far-infrared (terahertz) emitters is only beginning to be investigated.[3,4] At mid-IR wavelengths free-carrier absorption tends to dominate the internal loss, and at longer wavelengths it is critical in determining whether sufficient gain can be generated to achieve lasing at all.

In some classes of mid-IR semiconductor lasers, such as those featuring type-II antimonide quantum wells with large conduction-band offsets,[1] it is believed that cavity losses are dominated by intervalence absorption. However, once the lasing wavelength becomes longer than the smallest valence intersubband splitting, intervalence losses are virtually eliminated. Scattering-assisted absorption by free electrons and holes in the active quantum wells then usually determines the internal loss in optically pumped laser devices with undoped claddings. Even in electrically pumped devices, assisted free-carrier absorption (FCA) can dominate if the lasing mode is optically confined primarily to the active region, as in the interband cascade lasers.[5] FCA in diode optical cladding layers consisting of superlattice injectors[6,7] can also be significant. In general, for TE-polarized devices, scattering-assisted FCA tends to become more and more important with increasing wavelength.

The theory for FCA in bulk semiconductors[8–10] is well developed and verified experimentally. The effect of nonparabolicity on midinfrared absorption in III–V semiconductors has also been considered recently.[11] For the case of quantum wells, a number of papers have dealt with FCA of TE-polarized radiation assisted by acoustic[12] and polar optical[13–16] phonon scattering including the effects of phonon confinement,[17] piezoelectric coupling,[18] ionized impurities,[19,20] and electron-electron scattering.[21] Most of the previous works employed the infinite-well approximation, and often parabolic dispersion relations as well. Furthermore, quantitative comparison of those results with the absorption spectra of real quantum wells is often rather difficult. The results were usually compared with the bulk FCA, which is not always illuminating insofar as the mobility in the three-dimensional (3D) and quasi-2D systems can be very different.

Little work on scattering-assisted FCA of TM-polarized light in narrow quantum wells has been reported. The only (to our knowledge) published papers[18,22] on the topic considered primarily thick layers and only absorption due to the electron-phonon interaction. None of the previous articles have addressed the interesting issue of how the wavelength dependence of the absorption coefficient for a quasi-two-dimensional system makes a smooth transition between the quantum and semiclassical regimes.[23,24] In current practice, the semiclassical expression is usually used as the default for estimating FCA coefficients for quantum-well systems.

In this paper, we will calculate the FCA assisted by scattering from quantum-well interface fluctuations.[25–27] This interface roughness scattering is known to dominate the mobility in narrow wells at cryogenic temperatures.[26,28,29] This regime is precisely that of interest for far-infrared and terahertz semiconductor lasers, based on both intersubband and interband transitions.[3,4] Absorption coefficients will be calculated for the examples of GaAs/AlGaAs and InAs/AlSb quantum wells, as well as an antimonide *W* laser structure designed for terahertz emission. We will also consider in detail the applicability of the standard semiclassical approximation to these quantum well structures for a wide range of input parameters.

II. FORMALISM

A. TE-polarized absorption

As in all past works on the topic that we are aware of, band mixing in the sense of appreciable contributions of *p*-like zone-center Bloch functions to the conduction-band wave function will be neglected. (On the other hand, the

effect of other bands on the electron dispersion is included in the framework of the eight-band $\mathbf{k}\cdot\mathbf{p}$ theory.) The inclusion of that higher-order effect would considerably complicate the formalism due to the introduction of much different selection rules for electron scattering between conduction states with a valencelike character.[30]

The matrix element for absorption of TE-polarized (in the plane of the quantum well) light with both final and initial states in the conduction band is given by

$$\langle \mathbf{k}',n'|H_{\mathrm{RAD}}^{\mathrm{TE}}|\mathbf{k},n\rangle = \frac{e\hbar}{m_n^*(k)}\left(\frac{\hbar}{2\varepsilon V\omega}\right)^{1/2}\mathbf{e}\cdot\mathbf{k}\,\delta_{k',k}\delta_{n',n}, \tag{1}$$

where $\mathbf{k}$ and n are the momentum and subband index of the initial state, $\mathbf{k}'$ and n' are the corresponding quantities for the final state, the wave-vector-dependent inverse (velocity) effective mass $1/m_n^*(k)=(\partial E_n/\partial k)/(\hbar^2 k)=v_n/\hbar k$ is derived from numerically computed nonparabolic dispersion relations, $v_n(k)$ is the velocity, $\mathbf{e}$ is the unit polarization vector, ε (ω) is the dielectric constant, $\hbar\omega$ is the photon energy, and V is the normalization volume. Isotropic dispersion has been assumed for simplicity. Equation (1) allows only momentum-conserving intrasubband transitions. Since energy and momentum cannot be conserved simultaneously, there is no first-order contribution to the absorption coefficient for $\hbar\omega$ below the energy gap.

The second-order contribution is made possible by the presence of a symmetry-breaking scattering mechanism (multiphoton processes are not considered here). In second-order perturbation theory, the matrix element connecting the initial and final states for an optical transition in a quantum well is given by

$$\langle \mathbf{k}',n'|M|\mathbf{k},n\rangle = \sum_{\mathbf{k}'',m}\left[\frac{\langle \mathbf{k}',n'|H_{\mathrm{RAD}}|\mathbf{k}'',m\rangle\langle \mathbf{k}'',m|H_{\mathrm{IR}}|\mathbf{k},n\rangle}{E_n(\mathbf{k})-E_m(\mathbf{k}'')} + \frac{\langle \mathbf{k}',n'|H_{\mathrm{IR}}|\mathbf{k}'',m\rangle\langle \mathbf{k}'',m|H_{\mathrm{RAD}}|\mathbf{k},n\rangle}{E_n(\mathbf{k})-E_m(\mathbf{k}'')+\hbar\omega}\right], \tag{2}$$

where $\mathbf{k}''$ and m are the momentum and subband index of the intermediate state, and E_n ($\mathbf{k}$) and E_m ($\mathbf{k}''$) are the electron energies for the initial and intermediate state, respectively.

In particular we treat the case of photon absorption mediated by carrier scattering from interface roughness fluctuations, although many of the qualitative conclusions will be equally applicable to other scattering mechanisms. The matrix element for roughness scattering from a quantum-well interface can be approximated by the relation[26,28]

$$\langle \mathbf{k}',n'|H_{\mathrm{IR}}|\mathbf{k},n\rangle = \frac{\sqrt{\pi}\Lambda\Delta}{\sqrt{A}}\exp\left(-\frac{q^2\Lambda^2}{8}\right) \times\left[\frac{\partial E_{n'}(\mathbf{k}')}{\partial z}\right]^{1/2}\left[\frac{\partial E_n(\mathbf{k})}{\partial z}\right]^{1/2}, \tag{3}$$

where $\mathbf{q}=\mathbf{k}-\mathbf{k}'$, A is the normalization area, Λ is the roughness correlation length, and Δ is the fluctuation depth. The two derivatives are taken at the interface under consideration. Computing the total scattering rate involves summing the contributions from each interface. A more fundamental, but less practical, relation[25] reveals that Eq. (3) neglects the sign of the wave-function derivatives at the interfaces. A simple rule for correcting this deficiency required for intersubband scattering processes is to flip the sign of the matrix element whenever the two wave functions have derivatives with different signs. In this paper, we will be concerned primarily with relatively low carrier densities, which at low temperatures are sufficient to reach transparency and lasing. Screening effects are therefore expected to be small, and for simplicity we ignore them in the following discussion, although screening can be treated readily by an appropriate modification of Eq. (3).[26]

Using Eqs. (1) and (2), we can reduce the second-order matrix element for TE-polarized light to the following form:

$$\langle \mathbf{k}',n'|M|\mathbf{k},n\rangle = \frac{\langle \mathbf{k}',n'|H_{\mathrm{IR}}|\mathbf{k},n\rangle\langle \mathbf{k},n|H_{\mathrm{RAD}}^{\mathrm{TE}}|\mathbf{k},n\rangle - \langle \mathbf{k}',n'|H_{\mathrm{RAD}}^{\mathrm{TE}}|\mathbf{k}',n'\rangle\langle \mathbf{k}',n'|H_{\mathrm{IR}}|\mathbf{k},n\rangle}{\hbar\omega}. \tag{4}$$

The scattering rate from the initial state to the final state is then given by the golden rule:

$$W_{\mathbf{k},n;\mathbf{k}',n'} = \frac{2\pi}{\hbar}\sum_{\text{all interfaces}}|\langle \mathbf{k}',n'|M|\mathbf{k},n\rangle|^2 \times\delta(E_{n'}(\mathbf{k}')-E_n(\mathbf{k})-\hbar\omega). \tag{5}$$

The absorption coefficient is calculated by summing over all occupied initial states and unoccupied final states. Next, free-carrier emission is subtracted from the absorption coefficient. Inclusion of the emission contribution is critical to obtaining a correct result in the limit of very long wavelengths,[23] as will be shown below. Averaging over orthogonal in-plane polarizations yields a factor of $\frac{1}{2}$. The total absorption coefficient for TE-polarized light is finally given by

$$\alpha_{\mathrm{FCA}}^{\mathrm{TE}} = \frac{e^2\Lambda^2\Delta^2 n_m}{8\pi c\varepsilon d\omega^3}\sum_{\text{all int.}}\sum_n\int k\,dk\sum_{n'}\int k'\,dk' \times\int_0^{2\pi}d\theta\left[\frac{\partial E_n(\mathbf{k})}{\partial z}\right]\left[\frac{\partial E_{n'}(\mathbf{k}')}{\partial z}\right]\exp\left(\frac{-q^2\Lambda^2}{4}\right) \times\left(\frac{k^2}{m_n^{*2}(k)}+\frac{k'^2}{m_{n'}^{*2}(k')}-\frac{2kk'\cos\theta}{m_n^*(k)m_{n'}^*(k')}\right) \times(f_{n,\mathbf{k}}-f_{n',\mathbf{k}'})\,\delta(E_{n'}(\mathbf{k}')-E_n(\mathbf{k})-\hbar\omega), \tag{6}$$

where n_m is the modal refractive index and d is the period. Although several of the other terms also carry implicit wavelength dependences, e.g., through the energy of the final state, the explicit wavelength proportionality in Eq. (6) is cubic. This cubic dependence is expected to hold for *intrasubband* absorption of photons with energies much larger than k_BT for weakly nonparabolic carrier systems. The integral over final states can be eliminated using the energy-conserving delta function. It is interesting to note that elastic interface-roughness scattering in second-order theory takes place between states separated by the photon energy, whereas the photon-absorption portion of the interaction has effectively become elastic. This is due to the absence of any condition governing energy conservation in the intermediate state. Furthermore, the exclusion principle does not apply to intermediate states, which will be seen below to have interesting consequences for TM-polarized absorption.

The extension of the above formalism to hole FCA can be complicated owing to strong band mixing effects in the valence band. However, in the case of narrow gap materials, quantum confinement and, in some cases, compressive strain, lead to large splittings between the valence subbands and a hole mass that is not much larger than the electron effective mass. Therefore the presented formalism can be used to estimate the hole FCA coefficient in this regime for photon energies smaller than intervalence splittings.

In developing our formalism, we have so far ignored processes with intermediate states in the valence band. Above the energy gap, strong interband processes dominate TE-polarized absorption, and any second-order correction is likely to be negligible. Although second-order processes with intermediate states in the valence band can proceed when $\hbar\omega < E_g$, even for narrow gap semiconductors such as InAs, their contribution to the FCA coefficient is found to be quite small owing to the large denominators in Eq. (1). The issue of valence intermediate states will be examined more closely below in connection with antimonide ''*W*'' laser structures having energy gaps in the terahertz frequency range.

B. Connection with semiclassical formalism

In the limit of very long wavelengths, the absorption coefficient is known to reduce to the semiclassical form,[24] which scales as λ^2. This expression, which we will derive next, is semiclassical in that whereas the electron transport is handled quantum mechanically, the interaction of light with the electrons is treated using the classical Drude theory.

The semiclassical expression becomes a reasonable approximation in the limit of $k_BT \gg \hbar\omega$ for nondegenerate statistics or $E_F \gg \hbar\omega$ in the degenerate regime, where E_F is the Fermi energy. In those limits, $n'=n$, $\mathbf{k}' \approx \mathbf{k}$, $q^2 = 2k^2(1-\cos\theta)$, $f_{n,\mathbf{k}} - f_{n',\mathbf{k}'} \approx (\partial f_{n,\mathbf{k}}/\partial E)\hbar\omega$, and the absorption coefficient of Eq. (6) can be rewritten:

$$\alpha_{\mathrm{FCA}}^{\mathrm{SC}} = \frac{e^2 n_m}{c\varepsilon d\omega^2} \sum_n \int d^2k \frac{\partial f_{n,\mathbf{k}}}{\partial E} \frac{v^2}{2\tau_n(k)}, \tag{7}$$

where the average is over the inverse relaxation time:

$$\frac{1}{\tau_n(k)} = \frac{\Delta^2\Lambda^2}{2\hbar} \sum_{n'} \int k'dk' \int_0^{2\pi} d\theta (1-\cos\theta) \left[\frac{\partial E_n(\mathbf{k})}{\partial z}\right] \times \left[\frac{\partial E_{n'}(\mathbf{k}')}{\partial z}\right] \exp\left(\frac{-k^2\Lambda^2(1-\cos\theta)}{4}\right) \times \delta(E_{n'}(\mathbf{k}') - E_n(\mathbf{k})). \tag{8}$$

In this paper, we will refer to the quantity α^{SC} given by Eq. (7) as the semiclassical absorption coefficient. It displays the widely assumed quadratic dependence on the wavelength of the light. However, in the literature this is usually expressed in terms of the mobility μ:[31]

$$\alpha = \frac{Ne^3 n_m}{c\varepsilon d\omega^2 m^{*2}\mu}, \tag{9}$$

where N is the two-dimensional carrier density, and the mobility for an arbitrary in-plane direction is defined through the following relation:

$$\mu = \frac{e\langle\tau\rangle}{m^*} = \frac{e}{N} \sum_n \int d^2k \frac{\partial f_{n,\mathbf{k}}}{\partial E} \frac{v^2}{2} \tau_n(k). \tag{10}$$

Comparing Eq. (7) on the one hand with Eqs. (9) and (10) on the other, it should be clear that the semiclassical result represented by Eq. (9) is accurate only insofar as it is a good approximation to set $\langle\tau^{-1}\rangle = \langle\tau\rangle^{-1}$. While the approximate equality holds in many cases of interest including some of those considered in this paper, scattering processes for which the error is appreciable can easily be envisaged. In particular, the approximation is expected to become quite poor at elevated temperatures when FCA is mediated by a strongly energy-dependent scattering mechanism.

C. TM-polarized absorption

To derive analogous FCA formulas for the case of TM-polarized (optical electric field along the quantum-well growth direction) light, we consider the corresponding matrix element for the photon transition:

$$\langle \mathbf{k}', n' | H_{\mathrm{RAD}}^{\mathrm{TM}} | \mathbf{k}, n \rangle = \frac{[m_n^*(k) + m_{n'}^*(k)]e\hbar}{2m_n^*(k)m_{n'}^*(k)} \left(\frac{\hbar}{2\varepsilon V\omega}\right)^{1/2} \times \delta_{\mathbf{k}',\mathbf{k}} \int dz \Psi_{n',\mathbf{k}'}^* \frac{\partial}{\partial z} \Psi_{n,\mathbf{k}}. \tag{11}$$

Equation (11) shows that only transitions involving a change of parity are allowed. Because both momentum and energy can be conserved in parity-flipping intersubband transitions, strong first-order absorption may be expected near the intersubband resonances. Since those processes have already received considerable attention in the literature,[30,32] our task here will be to examine the second-order contributions and to determine their magnitudes for typical values of the carrier scattering rates relative to the well-known first-order intersubband absorption coefficients.

The second-order absorption coefficient for TM-polarized light has the same form as Eq. (6) except that we must keep the sum over all intermediate states in Eq. (1). An obvious difficulty is that for some processes the intermediate states

can be arbitrarily close in energy to the initial or final states, which results in singularities. This is circumvented in the usual manner[33] by introducing a broadening parameter Γ:

$$\langle \mathbf{k}',n'|M|\mathbf{k},n\rangle = \sum_{\mathbf{k}'',m}\left[\frac{\langle \mathbf{k}',n'|H_{\mathrm{RAD}}^{\mathrm{IM}}|\mathbf{k}'',m\rangle\langle \mathbf{k}'',m|H_{\mathrm{IR}}|\mathbf{k},n\rangle}{E_n(\mathbf{k})-E_m(\mathbf{k}'')+i\Gamma} + \frac{\langle \mathbf{k}',n'|H_{\mathrm{IR}}|\mathbf{k}'',m\rangle\langle \mathbf{k}'',m|H_{\mathrm{RAD}}^{\mathrm{TM}}|\mathbf{k},n\rangle}{E_n(\mathbf{k})-E_m(\mathbf{k}'')+\hbar\omega+i\Gamma}\right]. \tag{12}$$

The absorption coefficient is then proportional to the real part of the square of the matrix element, whereas the imaginary part gives rise to a small change of the refractive index.

The second-order absorption coefficient assisted by interface-roughness scattering [Eq. (12)] will be compared with the first-order intersubband absorption coefficient given by

$$\alpha_{TM}^{(1)} = \frac{n_m \pi e^2 \hbar^2}{c\varepsilon\omega d}\sum_n \int kdk \sum_{n'} \frac{m_n^*(k)+m_{n'}^*(k')}{2m_n^*(k)m_{n'}^*(k')} \times\left[\int dz \Psi_{n',\mathbf{k}'}^* \frac{\partial}{\partial z}\Psi_{n,\mathbf{k}}\right]^2 (f_{n,\mathbf{k}}-f_{n',\mathbf{k}'}) \times \delta_{\mathbf{k},\mathbf{k}'}\delta[E_{n'}(\mathbf{k}')-E_n(\mathbf{k})-\hbar\omega]. \tag{13}$$

In deriving Eq. (13) care was taken to preserve the symmetric form of the interaction Hamiltonian, which is necessary to take into account the different effective masses of the initial and final states.[30] In order to compare the first-order absorption coefficient of Eq. (13) with the second-order FCA coefficient, we follow the standard procedure and substitute a Lorentzian line-shape function for the delta function in Eq. (13). Although the prescription for the introduction of line broadening is different in the FCA expression, this should provide a reasonable first-order estimate of the relative importance of the first-order and second-order contributions.

III. RESULTS

A. TE-polarized absorption in GaAs/AlGaAs wells

We begin by considering the simple case of free-electron absorption in a single 100-Å $GaAs/Al_{0.35}Ga_{0.65}As$ quantum well. The band structure and wave functions for this and all of the following examples were computed using an eight-band $\mathbf{k}\cdot\mathbf{p}$ model based on a finite-element technique.[34] The TE-polarized quantum FCA coefficient obtained using Equation (6) is shown as a function of wavelength in Fig. 1 for a sheet carrier density of $N=10^{11}\,\mathrm{cm}^{-2}$ at $T=10\,\mathrm{K}$, and assuming monolayer fluctuations. A change in the width of the quantum well by $\Delta=1$ ML results in 0.52-, 1.83-, and 3.01-meV shifts for the first, second, and third subband energies, respectively. Generally speaking, narrower quantum wells will have higher absorption coefficients owing to larger energy shifts with the precise scaling determined by the barrier height and effective mass. In Fig. 1, the results are given for roughness correlation lengths of $\Lambda=70$ Å (solid line) and 30 Å (dashed line), which are typical of the observed range.[26] These parameters imply low-temperature, low-density mobilities of $2.3\times10^4\,\mathrm{cm}^2/\mathrm{Vs}$ and $1.0\times10^5\,\mathrm{cm}^2/\mathrm{Vs}$, respectively. For simplicity, we neglect the strong variation of the refractive index near the edges of the Reststrahlen phonon band, which lies between $\lambda\approx34$ and 37 μm in GaAs and at slightly shorter wavelengths in AlAs. Light in this wavelength range undergoes nearly total reflection from the surface of the sample. Similarly, the plasma contribution to the refractive index is neglected.

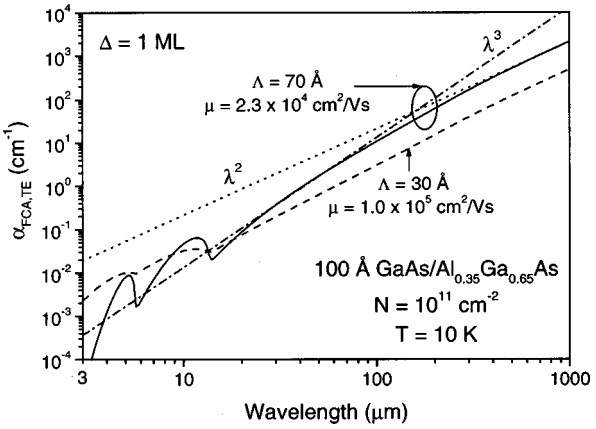

FIG. 1. Free-carrier absorption coefficient as a function of wavelength for TE-polarized light incident on a 100-Å $GaAs/Al_{0.35}Ga_{0.65}As$ quantum well with a carrier density of $10^{11}\,\mathrm{cm}^{-2}$ at a temperature of 10 K. Scattering from monolayer fluctuations at the interfaces is the mediating mechanism, and the FCA coefficient is shown for roughness correlation lengths of 70 Å (solid line, corresponding to a mobility of $2.3\times10^4\,\mathrm{cm}^2/\mathrm{Vs}$) and 30 Å (dashed line, $\mu=1.0\times10^5\,\mathrm{cm}^2/\mathrm{Vs}$). For the former case, the semiclassical quadratic (dotted) and cubic (dash-dotted) fits are also shown.

Also plotted in Fig. 1 are the semiclassical (with a λ^2 wavelength dependence) absorption coefficient [Eq. (7)] (dotted line) and a λ^3 fit to the quantum FCA coefficient in the intermediate wavelength range (dash-dotted line) for the case of $\Lambda=70$ Å. The quantum absorption coefficient is seen to converge to the semiclassical value as the wavelength increases beyond 100 μm. This is due to the relatively small Fermi energy above the band edge (corresponding to 500 μm) and low temperature. For shorter wavelengths, which are more often of practical importance, the quantum $\alpha_{\mathrm{FCA,TE}}$ is significantly lower than the semiclassical result. In fact, in the range between $\lambda\approx25$ and 70 μm, with the exception of the vicinity of the Reststrahlen band, the absorption coefficient is very well fit by the cubic wavelength dependence, explicit in Eq. (6). These results are directly analogous to the distinct regimes in the wavelength dependence of the bulk FCA coefficient, which have been well known for some time.[35]

The two features at 13 and 5.6 μm correspond to the 1-2 and 1-3 subband separations, respectively. When the photon energy becomes large enough to allow transitions to higher subbands, the absorption strength is increased substantially since higher subbands are more strongly perturbed by interface fluctuations. The enhancement of the absorption coefficient associated with scattering to higher subbands also holds for other scattering mechanisms such as polar optical-phonon scattering.[13]

The correlation length of interface disorder is a parameter that depends on the growth conditions. Changes in the cor-

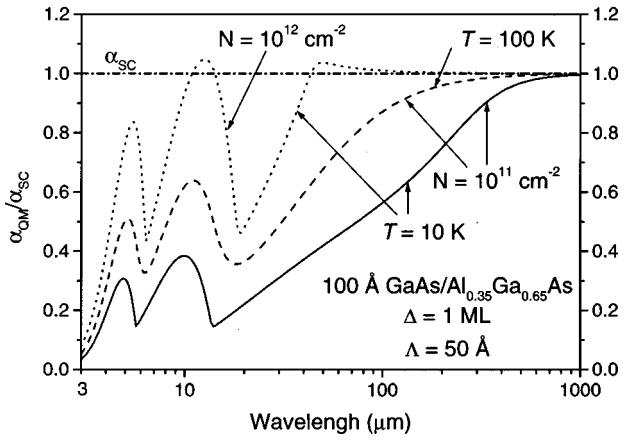

FIG. 2. Ratio between roughness-assisted quantum and semiclassical FCA coefficients as a function of wavelength for TE-polarized light incident on a 100-Å $GaAs/Al_{0.35}Ga_{0.65}As$ quantum well. Monolayer fluctuations and a correlation length of 50 Å are assumed. The ratio is shown for carrier densities of $10^{11}\,cm^{-2}$ at temperatures of 10 K (solid line) and 100 K (dashed line) and $10^{12}\,cm^{-2}$ at $T=10\,K$ (dotted line).

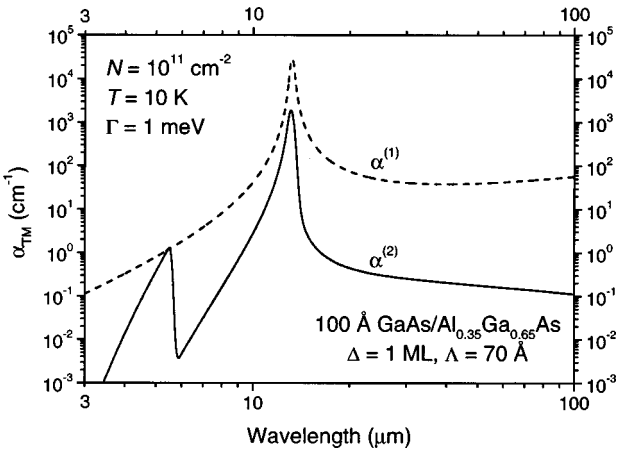

FIG. 3. Roughness-assisted second-order (solid line) and intersubband first-order (dashed line) absorption coefficient vs wavelength for TM-polarized light incident on a 100-Å $GaAs/Al_{0.35}Ga_{0.65}As$ quantum well with a carrier density of $10^{11}\,cm^{-2}$ at a temperature of 10 K. Monolayer fluctuations, a correlation length of 50 Å, and a broadening linewidth of 1 meV are assumed in both cases.

relation length can significantly modify the low-temperature mobility. Since the Fermi wave vector in the case considered in Fig. 1 is rather small, a reduction in the roughness correlation length leads to a higher mobility. The semiclassical expression predicts an absorption coefficient roughly inversely proportional to the mobility [Eq. (9)]. However, it is clear from Fig. 1 that at wavelengths shorter than 9 μm the absorption coefficient is actually *reduced* for a larger correlation length and lower mobility, which is opposite to the prediction of the semiclassical theory. In fact, in order to understand this effect, one should recall that the semiclassical expression takes into consideration only elastic carrier scattering near the bottom of the subband, for which $q_{max}=2k_F$. However, it is clear from the quantum theory that in order to absorb a short-wavelength photon, electrons must be scattered to states far above the band edge. In this case, the momentum transfer is quite large, and the exponential dependence dominates the scattering matrix element in Eq. (3). Thus a large correlation length acts to suppress short-wavelength absorption in spite of the reduced low-field mobility.

For nondegenerate carrier densities, the absorption coefficient scales with N, while its spectral shape remains essentially invariant. However, as the carrier density becomes degenerate, the functional dependence deviates from linear at longer wavelengths due to the increased occupation of final states. A similar effect reduces the absorption coefficient for $\lambda>100\,\mu$m at higher temperatures. Both the quantum and semiclassical expressions reproduce these exclusion effects. Therefore in Fig. 2 we plot the *ratio* between the coefficients obtained by using Eqs. (6) and (7) for a carrier density of $N=10^{11}\,cm^{-2}$ at temperatures of 10 K (solid line) and 100 K (dashed line) and $N=10^{12}\,cm^{-2}$ at $T=10\,K$. It is clear that as either the temperature or degeneracy is increased, better agreement with the semiclassical expression at shorter wavelengths is obtained. However, for scattering to higher subbands, the quantum absorption coefficient can actually exceed the semiclassical value owing to the stronger perturbation of the subband energies. At room temperature, both the mobility and the FCA are likely to be dominated by optical-phonon scattering rather than the interface roughness scattering treated here. While the details of the absorption spectrum will depend on the dominant scattering mechanism, the main qualitative features treated in Figs. 1 and 2 should remain valid, especially for elastic (or nearly elastic on the scale of the photon energy) processes. Absorption enhancement is expected whenever the photon energy is large enough to permit scattering to higher subbands. For most collision mechanisms, the intrasubband scattering rate declines as the difference between the energies of the initial state and the final state increases. If this is so, the semiclassical approximation is expected to overestimate the absorption coefficient by analogy with the results of this subsection.

Another interesting extension of these quantum-well results would be to superlattices with nonzero dispersion along the growth direction. In the superlattice case, conservation of crystal momentum along the growth axis for radiative transitions must be enforced. Therefore a smooth transition to the 3D regime is expected as the width of the miniband increases (interminiband TE-polarized radiative transitions are forbidden in lowest order).

B. TM-polarized absorption in GaAs/AlGaAs wells

So far, we have considered FCA of TE-polarized light. However, the GaAs well is also capable of strong second-order absorption of light propagating with TM polarization. In this case, we will compare the strength of second-order absorption assisted by interface roughness scattering to first-order intersubband absorption assuming the same broadening linewidth of $\Gamma=1$ meV and a Lorentzian line shape. The comparatively small linewidth is adopted in order to emphasize the relative strengths of the two mechanisms.

In Fig. 3, we plot the second-order (solid line) and first-order (dashed line) absorption coefficients for TM polarization as a function of wavelength for $N=10^{11}\,cm^{-2}$ and $\Lambda=70\,$Å. We noted in connection with Eq. (13) that a change

of parity is required for first-order intersubband absorption. Thus no first-order absorption from the first subband to the third subband can take place, although $\alpha_{\mathrm{TM}}^{(1)}$ ($\hbar\omega = E_{13}$) is nonzero owing to broadening and nonparabolicity. On the other hand, second-order 1-3 absorption can proceed via an intermediate state in the second subband. This mechanism is primarily responsible for the peak at 5.6 μm, which slightly exceeds the broadened first-order absorption coefficient at this wavelength. Nonetheless, the combined absorption coefficient remains rather small (a few cm^{-1}).

The second peak at 13 μm corresponds to the ''allowed'' 1-2 intersubband absorption process. The second-order absorption coefficient is over 2000 cm^{-1}, but represents at most 18% of the first-order peak. It is interesting to note that the relative strength of the second-order process peaks near E_{12}, which reflects the higher scattering rate for states near the bottom of the respective subbands.

While the results of Fig. 3 are for a particular case of scattering from monolayer fluctuations, mediating processes that produce second-order absorption coefficients similar to or greater than the first-order coefficients, such as scattering from interface fluctuations that are several monolayers deep or polar optical phonon scattering at high temperatures, are also possible. In general, these mechanisms will also have a much more severe impact on the mobility.

Since the exclusion principle can be disregarded for intermediate states, it would appear that second-order absorption through intermediate states in the occupied second subband with initial and final states in the first subband could in principle take place. However, in practice this effect is counterbalanced by the second-order contribution to intersubband gain with initial states in the second subband and final states in the first subband. The overall effect encompassing all second-order contributions is a small enhancement of the gain cross section for the inverted intersubband transition.

The extension of the present results to superlattices should be treated with more care than for TE-polarized FCA. A generalization of Eq. (11) reveals the existence of two terms, the first accounting for interminiband transitions analogous to intersubband transitions, and the second of the form of Eq. (1) with conservation of all three components of the crystal momentum. As the miniband width is increased, the first term vanishes, while the second converges to the bulk expression. The second term should have a small contribution to the total transition probability when the photon energy is smaller than the difference between the top of the miniband and the Fermi energy. Therefore the general conclusions of this subsection apply for the wavelength range of interest in many practical superlattice systems.

C. FCA in antimonide quantum wells

So far our examples have employed the GaAs/AlGaAs material system, which has a relatively large electron effective mass, weak nonparabolicity, and a small conduction-band offset. It is interesting to compare the foregoing results with those for InAs/AlSb quantum wells, which have a smaller effective mass (that enhances the effects of interface fluctuations), much stronger nonparabolicity, and a much higher conduction-band offset that allows transitions between confined states at shorter wavelengths.

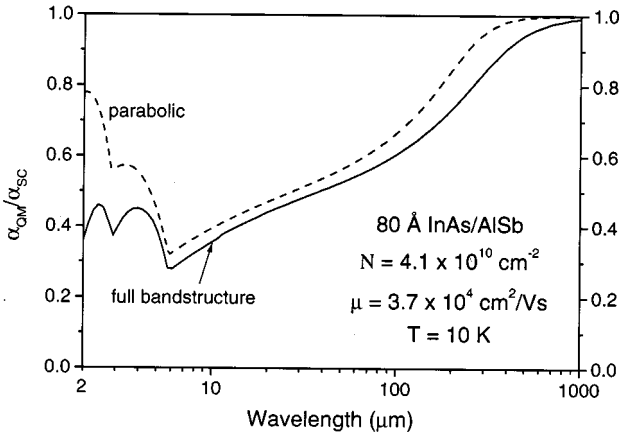

FIG. 4. Free-carrier absorption coefficient obtained using the full band structure (solid line) and the parabolic approximation (dashed line) as a function of wavelength for TE-polarized light incident on an 80-Å InAs/AlSb quantum well with a carrier density of $4.1\times10^{10}\,\mathrm{cm}^{-2}$ and a mobility of $3.7\times10^{4}\,\mathrm{cm}^2/\mathrm{Vs}$ at $T=10\,\mathrm{K}$.

In Fig. 4, we show the ratio between the quantum and semiclassical TE-polarized absorption coefficients for an 80-Å InAs/AlSb square well with a carrier density of $4\times10^{10}\,\mathrm{cm}^{-2}$. The second and third subbands are separated from the first subband by energies of 217 and 442 meV, respectively, and the energy shifts of the first three subbands due to a 1-ML fluctuation are 2.16, 5.04, and 7.53 meV, respectively. A correlation length of 20 Å has been assumed, which results in a mobility of $3.7\times10^{4}\,\mathrm{cm}^2/\mathrm{Vs}$ at 10 K that is consistent with experimental results.[36,37] A larger correlation length was inferred in Ref. 37, possibly because of the simple band-structure model employed in that paper. For comparison, the same quantity is plotted in Fig. 4 assuming parabolic dispersion relations with the same carrier density and mobility (this requires Λ to be increased to 37 Å). The absorption coefficient for the parabolic approximation is seen to be overestimated over the entire spectral range, with the error being especially severe at the shortest wavelengths. The parabolic approximation also yields a semiclassical absorption coefficient that is too large, which results in a total error by a factor of 3–5 in the absolute value of α. It must be concluded that nothing short of a fully quantum description incorporating nonparabolicity in a detailed band-structure calculation is adequate to treat TE-polarized absorption in InAs/AlSb quantum wells. Results for the absorption of TM-polarized light are qualitatively similar to the case of the GaAs/AlGaAs quantum well.

We proposed[4] recently that for operation in the terahertz spectral range, antimonide interband optically pumped lasers may be advantageous over the intersubband quantum cascade laser.[2] Since the intervalence absorption that dominates the internal loss at mid-IR wavelengths[38,39] becomes negligible at very long λ, the FCA mechanism described in this paper is expected to dominate the internal loss in a terahertz interband laser emitting TE-polarized light. Here we test the semiclassical approximation used to derive the internal loss in our earlier analysis.[4]

We consider a 72.5-Å InAs/30-Å GaSb/62.5-Å InAs/65-Å AlSb *W* (Ref. 40) structure from Ref. 4 that was designed for the suppression of nonradiative recombination and for lasing

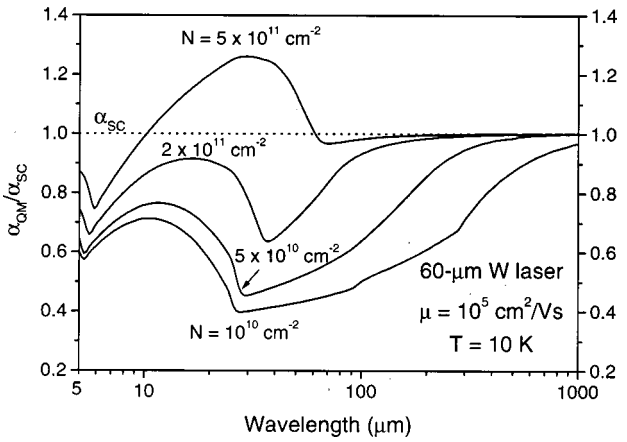

FIG. 5. Free-carrier absorption coefficient as a function of wavelength for TE-polarized light incident on a 72.5-Å InAs/30-Å GaSb/62.5-Å InAs/65-Å AlSb *W* structure with a mobility of $\approx 10^5$ cm^2/Vs (roughness correlation length of 20 Å) at $T=10$ K for several indicated carrier densities.

$\lambda \approx 60\,\mu$m. The double-electron-well geometry results in two closely spaced conduction subbands, whose splitting is increased to 50 meV by the slight asymmetry of the 72.5 and 62.5 Å well thicknesses. While no measurements of mobilities in such *W* structures have been performed, a magnetotransport analysis of InAs/GaInSb superlattices with similar electron-well widths indicated a low-temperature mobility on the order of 10^5 cm^2/Vs.[29] This mobility is obtained if we assume a correlation length of $\Lambda = 20$ Å for this *W* structure. It should be emphasized that, unlike the preceding cases of square quantum wells, contributions from interface roughness scattering at all four interfaces must be added here.

In Fig. 5, we plot the ratio between the quantum and semiclassical absorption coefficients for several carrier densities at 10 K. The inflection points corresponding to the onset of scattering to higher subbands are seen to be redshifted as the carrier degeneracy increases. For sheet densities less than 3×10^{11} cm^{-2}, the quantum absorption coefficient is smaller than the semiclassical value for all wavelengths of interest. In particular, we find that for the predicted threshold carrier density of 3.6×10^{10} cm^{-2}, the quantum-mechanical evaluation yields an absorption coefficient at $\lambda = 60\,\mu$m that is lower by approximately a factor of 2. The results for free-hole absorption should be similar since the electron and hole masses are nearly equal for this structure, although the hole absorption coefficient is slightly smaller because the hole mass is slightly larger. Thus the semiclassical calculation employed in Ref. 4 was somewhat conservative.

In calculating the absorption coefficients for Fig. 5, we have ignored the contributions from intermediate states in the valence band. In cases where $E_g \gg \hbar\omega$, this approximation is justified by the large denominator in Eq. (1) that results for such transitions. In the present example, we must be more careful because the type-II band gap is very small and corresponds to $\lambda = 60\,\mu$m. However, the reduction of the interband optical matrix element due to its indirect spatial nature, in combination with the weaker effect of interface roughness on the hole mobility, leads to a correction of only about 10% to the results presented in Fig. 5. This correction should be no larger than the error incurred in omitting band mixing-induced processes. It was predicted in Ref. 4 that it should be possible to obtain sufficient first-order interband gain to overcome the calculated FCA losses and permit lasing at low temperatures.

IV. CONCLUSIONS

We have considered free-carrier absorption of TE- and TM-polarized infrared light assisted by scattering from interface fluctuations in several technologically important quantum well structures. For the case of TE-polarized light, we have carried out a detailed comparison of our fully quantum-mechanical calculations with the predictions of the semiclassical theory and found considerable disagreement at wavelengths shorter than the reduced Fermi energy and also for transitions to higher subbands. An interesting finding is that for low carrier density and low temperature, the semiclassical expression usually tends to *overestimate* the absorption coefficient, in some cases by as much as a factor of 2.

The second-order absorption of TM-polarized light produces a rather small correction to the results obtained with first-order theory, in spite of the ''allowed'' nature of some transitions forbidden to first order by symmetry and exclusion arguments. This finding is important for validation of the calculations of internal loss in mid-IR intersubband semiconductor lasers, such as the quantum cascade laser (QCL). In the case of intersubband emission at terahertz frequencies, the wells become too wide to be sensitive to interface roughness. Assuming a temperature low enough to neglect phonon emission, the dominant nonradiative mechanism in these structures is expected to be intersubband relaxation by electron-electron scattering.[3] The latter mechanism can mediate free-electron absorption only when the dispersion relations are nonparabolic.[21] Active-region FCA in arsenide-based QCL's is therefore probably small even at terahertz frequencies, although the tendency toward substantial internal loss in the doped cladding layers must still be overcome.

ACKNOWLEDGMENTS

This work was supported by the Office of Naval Research. We are grateful to L. R. Ram-Mohan for useful discussions and to Quantum Semiconductor Algorithms for permission to use the finite-element software.

[1] I. Vurgaftman, C. L. Felix, and J. R. Meyer, in *Handbook of Thin Film Device Technology and Applications* (Academic, New York, in press).

[2] A. Tredicucci, F. Capasso, C. Gmachl, D. L. Sivco, A. L. Hutchinson, and A. Y. Cho, Appl. Phys. Lett. **73**, 2101 (1998).

[3] M. Rochat, J. Faist, M. Beck, U. Oesterle, and M. Illegems, Appl. Phys. Lett. **73**, 3724 (1998).

[4] I. Vurgaftman and J. R. Meyer, Appl. Phys. Lett. **75**, 899 (1999).

[5] L. J. Olafsen, E. H. Aifer, I. Vurgaftman, W. W. Bewley, C. L. Felix, D. Zhang, C.-H. Lin, and S. S. Pei, Appl. Phys. Lett. **72**,

2370 (1998).
[6] R. H. Miles, D. H. Chow, Y.-H. Zhang, P. D. Brewer, and R. G. Wilson, Appl. Phys. Lett. **66**, 1921 (1995).
[7] W. W. Bewley, E. H. Aifer, C. L. Felix, I. Vurgaftman, J. R. Meyer, C.-H. Lin, S. J. Murry, D. Zhang, and S.-S. Pei, Appl. Phys. Lett. **71**, 3607 (1997).
[8] H. Y. Fan, W. Spitzer, and R. J. Collins, Phys. Rev. **101**, 566 (1956).
[9] H. J. G. Meyer, Phys. Rev. **112**, 298 (1958).
[10] R. Rosenberg and M. Lax, Phys. Rev. **112**, 843 (1958).
[11] G. Shkerdin, J. Stiens, and R. Vounckx, J. Appl. Phys. **85**, 3792 (1999).
[12] H. N. Spector, Phys. Rev. B **28**, 971 (1983).
[13] H. Adamska and H. N. Spector, J. Appl. Phys. **56**, 1123 (1984).
[14] C. Trallero Giner and M. Anton, Phys. Status Solidi B **133**, 563 (1986).
[15] V. L. Gurevich, D. A. Parshin, and K. E. Shtengel, Fiz. Tverd. Tela (Leningrad) **30**, 1466 (1988) [Sov. Phys. Solid State **30**, 845 (1988)].
[16] C.-C. Wu and C.-J. Lin, J. Appl. Phys. **79**, 781 (1996).
[17] J. S. Bhat, B. G. Mulimani, and S. S. Kubakaddi, Phys. Status Solidi B **182**, 119 (1994).
[18] C.-C. Wu and C.-J. Lin, J. Phys.: Condens. Matter **6**, 10 147 (1994).
[19] N. S. Sankeshwar, S. S. Kubakaddi, and B. G. Mulimani, Pramana **32**, 149 (1989).
[20] F. M. Gashimzade and E. V. Tahirov, Phys. Status Solidi B **160**, K177 (1990).
[21] G. G. Zegrya and V. E. Perlin, Fiz. Tekh. Poluprovodn. **32**, 466 (1998) [Semiconductors **32**, 417 (1998)].
[22] C.-C. Wu and C.-J. Lin, Physica B **264**, 208 (1999).
[23] W. P. Dumke, Phys. Rev. B **124**, 1813 (1961).
[24] B. Jensen, Ann. Phys. (N.Y.) **95**, 229 (1975).
[25] R. E. Prange and T. W. Nee, Phys. Rev. **168**, 779 (1968).
[26] H. Sakaki, T. Noda, K. Hirakawa, M. Tanaka, and T. Matsusue, Appl. Phys. Lett. **51**, 1934 (1987).
[27] J. R. Meyer, D. J. Arnold, C. A. Hoffman, F. J. Bartoli, and L.-R. Ram-Mohan, Phys. Rev. B **46**, 4139 (1992).
[28] A. Gold, Solid State Commun. **60**, 531 (1986); Phys. Rev. B **35**, 723 (1987).
[29] C. A. Hoffman, J. R. Meyer, E. R. Youngdale, F. J. Bartoli, and R. H. Miles, Appl. Phys. Lett. **63**, 2210 (1993).
[30] R. Q. Yang, J. M. Xu, and M. Sweeny, Phys. Rev. B **50**, 7474 (1994).
[31] See, e.g., D. K. Schroder, R. N. Thomas, and J. C. Swartz, IEEE Trans. Electron Devices **25**, 254 (1978).
[32] L. C. West and S. J. Eglash, Appl. Phys. Lett. **46**, 1156 (1985).
[33] J. J. Sakurai, *Modern Quantum Mechanics* (Addison-Wesley, Reading, MA, 1994), revised ed., p. 333.
[34] L. R. Ram-Mohan and J. R. Meyer, J. Nonlinear Opt. Phys. Mater. **4**, 191 (1995).
[35] See, e.g., K. Seeger, *Semiconductor Physics: An Introduction* (Springer, New York, 1997), 6th ed.
[36] C. R. Bolognesi, H. Kroemer, and J. H. English, J. Vac. Sci. Technol. B **10**, 877 (1992).
[37] C. R. Bolognesi, H. Kroemer, and J. H. English, Appl. Phys. Lett. **61**, 213 (1992).
[38] W. W. Bewley, I. Vurgaftman, C. L. Felix, J. R. Meyer, C.-H. Lin, D. Zhang, S. J. Murry, S.-S. Pei, and L. R. Ram-Mohan, J. Appl. Phys. **83**, 2384 (1998).
[39] W. W. Bewley, C. H. Felix, E. H. Aifer, I. Vurgaftman, L. J. Olafsen, J. R. Meyer, H. Lee, R. U. Martinelli, J. C. Connolly, A. R. Sugg, G. H. Olsen, M. J. Yang, B. R. Bennett, and B. V. Shanabrook, Appl. Phys. Lett. **73**, 3833 (1998).
[40] J. R. Meyer, C. A. Hoffman, F. J. Bartoli, and L. R. Ram-Mohan, Appl. Phys. Lett. **67**, 757 (1995).